# Supporting information - WFOT: a WaveFunction Overlap Tool Between Single- and Multi-Reference Electronic Structure Methods for Spectroscopy Simulation

Alessandro Loreti,[†] Victor Manuel Freixas,[‡] Davide Avagliano,[†,#] Francesco Segatta,[†] Huajing Song,[¶,@] Sergei Tretiak,[¶,§] Shaul Mukamel,[‡] Marco Garavelli,[*,†] Niranjan Govind,[*,‖,⊥] and Artur Nenov[*,†]

†*Dipartimento di Chimica Industriale "Toso Montanari", University of Bologna, Via Piero Gobetti 85, 40129, Bologna, Italy*

‡*Department of Chemistry and Department of Physics and Astronomy, University of California, Irvine, 92697, USA*

¶*Physics and Chemistry of Materials, Theoretical Division, Los Alamos National Laboratory, Los Alamos, NM 87545, USA*

§*Center for Integrated Nanotechnologies, Los Alamos National Laboratory, Los Alamos, NM 87545, USA*

‖*Physical and Computational Sciences Directorate, Pacific Northwest National Laboratory, Richland, WA 99352*

⊥*Department of Chemistry, University of Washington, Seattle, WA 98195, USA*

#*Present address: Institute of Chemistry for Life and Health Sciences (I-CLEHS) Chimie Paristech, 11 Rue Pierre et Marie Curie, 75005, Paris, France*

@*Present address: Materials and Process Engineering, Pratt and Whitney, Raytheon Technologies, East Hartford, CT 06118, USA*

E-mail: marco.garavelli@unibo.it; niri.govind@pnnl.gov; artur.nenov@unibo.it

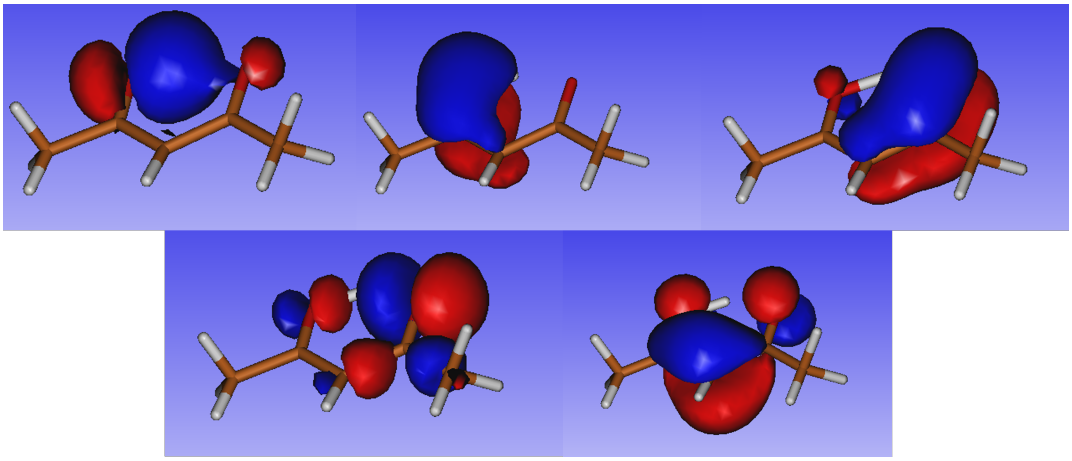

Supplementary Figure 1: Occupied molecular orbitals of the XMS-CASPT2 active space.

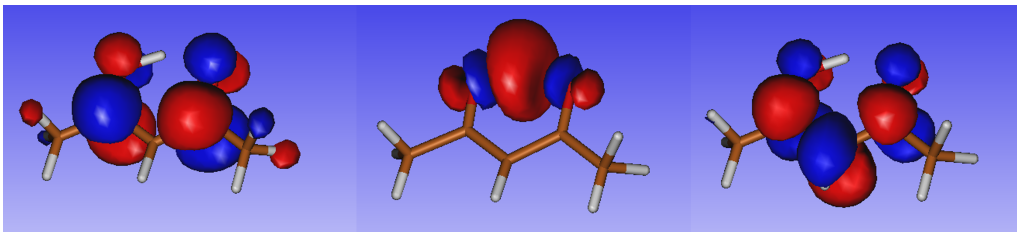

Supplementary Figure 2: Virtual molecular orbitals of the XMS-CASPT2 active space.

# Sample 3

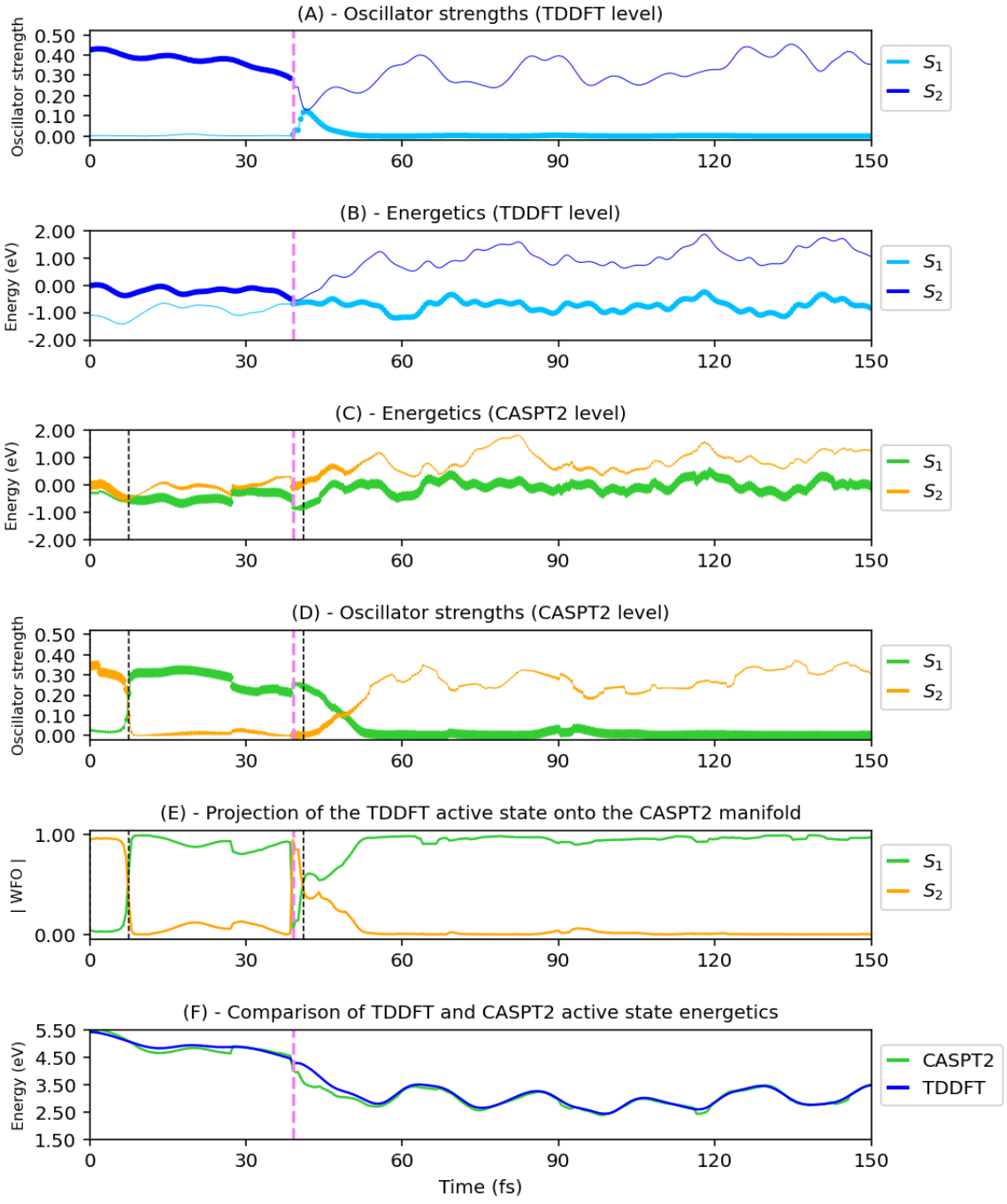


Supplementary Figure 3: Sample 3 - (A) Oscillator strengths of the two lowest excited states over the TD-DFT dynamic, highlighting the active one. (B) Energy of the three lowest excited states over the TD-DFT dynamic, highlighting the active one. (C) Energy of the two lowest excited states at CASPT2 level along the TD-DFT dynamic, highlighting the one with the highest overlap to the TD-DFT active state. (D) Oscillator strengths of the two lowest excited states at CASPT2 level over the TD-DFT dynamic, highlighting the one with the highest overlap to the TD-DFT active state; (E) Absolute value of the wavefunction overlap of the first two CASPT2 excited states with the TD-DFT active state. (F) Energy difference between active and ground state, computed at each level of theory. A fixed shift has been applied to account for the TDDFT overestimation of the $\pi\pi^*$ state energy. The line thickness in (C) and (D) is proportional to the projection of the TDDFT active state onto the CASPT2 manifold (E).

# Sample 4

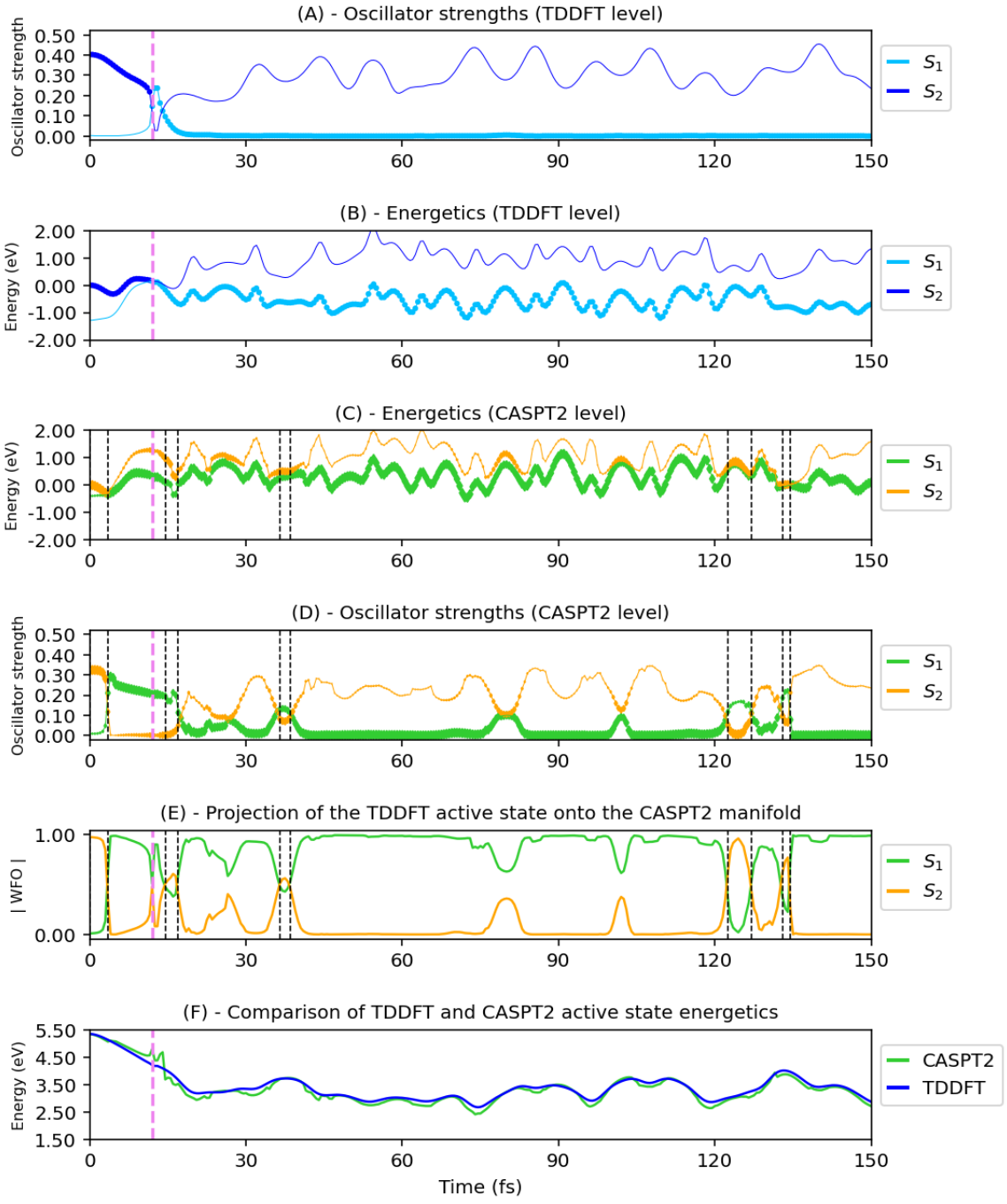


Supplementary Figure 4: Sample 4 - (A) Oscillator strengths of the two lowest excited states over the TD-DFT dynamic, highlighting the active one. (B) Energy of the three lowest excited states over the TD-DFT dynamic, highlighting the active one. (C) Energy of the two lowest excited states at CASPT2 level along the TD-DFT dynamic, highlighting the one with the highest overlap to the TD-DFT active state. (D) Oscillator strengths of the two lowest excited states at CASPT2 level over the TD-DFT dynamic, highlighting the one with the highest overlap to the TD-DFT active state; (E) Absolute value of the wavefunction overlap of the first two CASPT2 excited states with the TD-DFT active state. (F) Energy difference between active and ground state, computed at each level of theory. A fixed shift has been applied to account for the TDDFT overestimation of the $\pi\pi^*$ state energy. The line thickness in (C) and (D) is proportional to the projection of the TDDFT active state onto the CASPT2 manifold (E).

# Sample 5

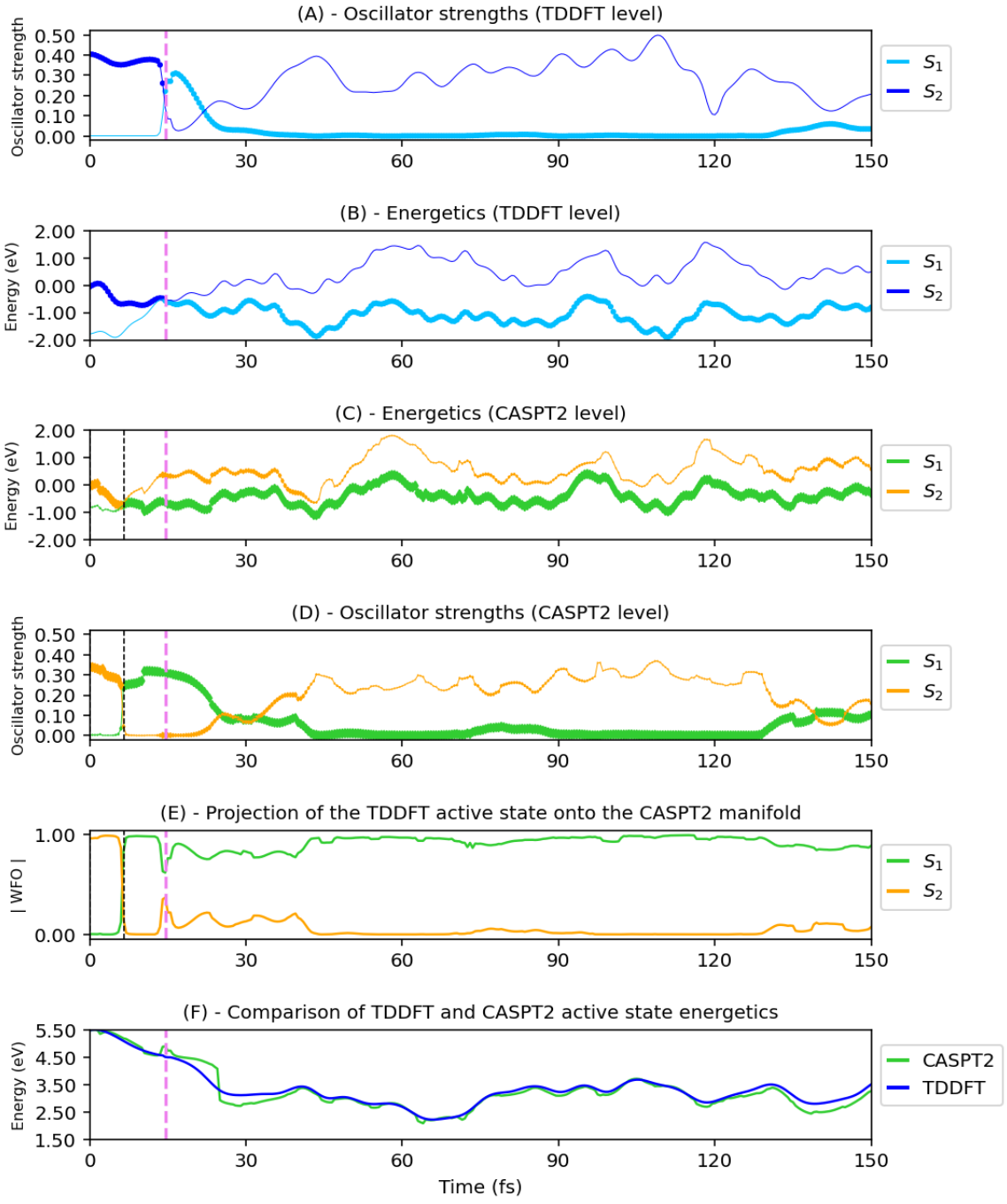


Supplementary Figure 5: Sample 5 - (A) Oscillator strengths of the two lowest excited states over the TD-DFT dynamic, highlighting the active one. (B) Energy of the three lowest excited states over the TD-DFT dynamic, highlighting the active one. (C) Energy of the two lowest excited states at CASPT2 level along the TD-DFT dynamic, highlighting the one with the highest overlap to the TD-DFT active state; (D) Oscillator strengths of the two lowest excited states at CASPT2 level over the TD-DFT dynamic, highlighting the one with the highest overlap to the TD-DFT active state. (E) Absolute value of the wavefunction overlap of the first two CASPT2 excited states with the TD-DFT active state. (F) Energy difference between active and ground state, computed at each level of theory. A fixed shift has been applied to account for the TDDFT overestimation of the $\pi\pi^*$ state energy. The line thickness in (C) and (D) is proportional to the projection of the TDDFT active state onto the CASPT2 manifold (E).

# Sample 6

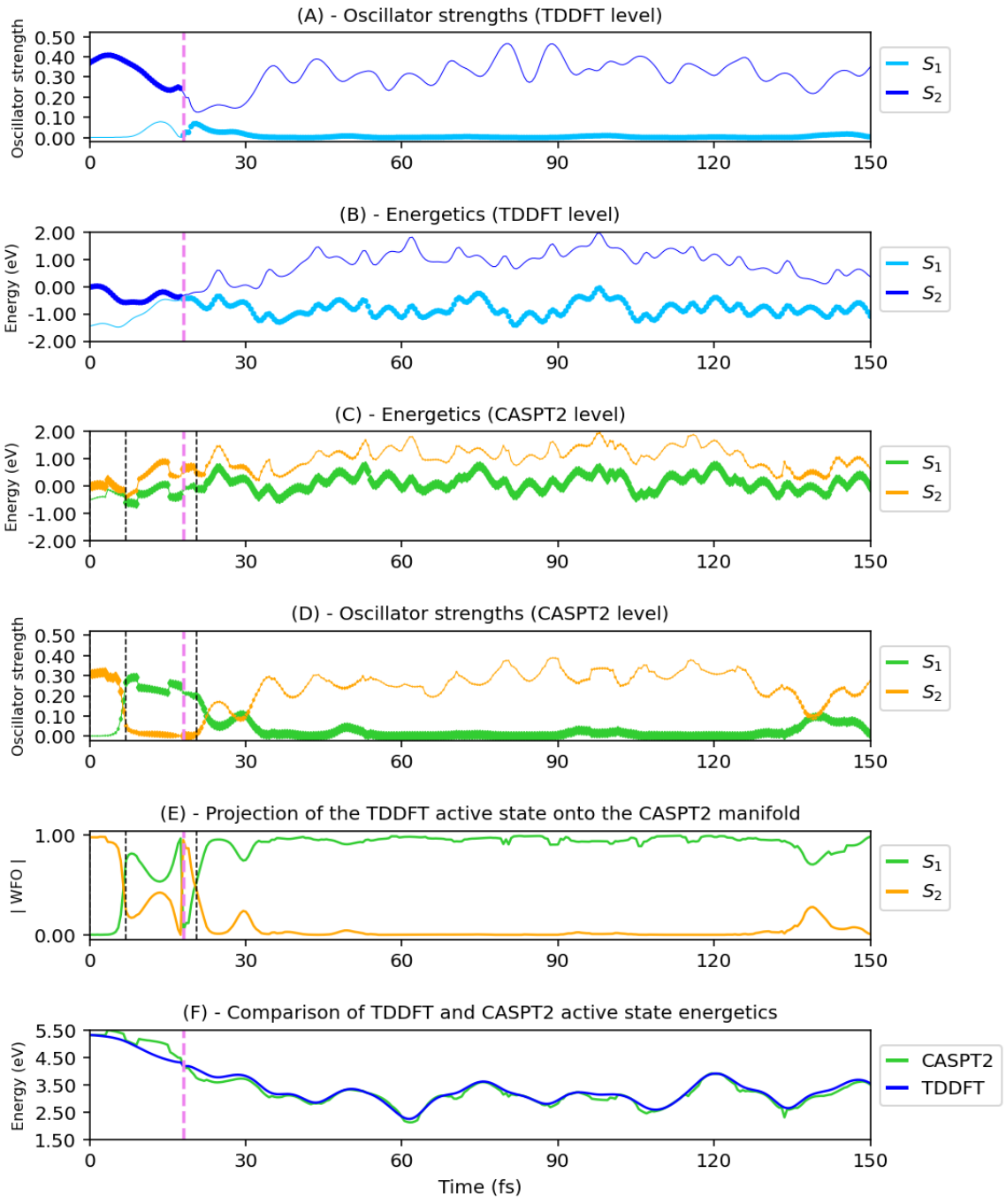


Supplementary Figure 6: Sample 6 - (A) Oscillator strengths of the two lowest excited states over the TD-DFT dynamic, highlighting the active one. (B) Energy of the three lowest excited states over the TD-DFT dynamic, highlighting the active one. (C) Energy of the two lowest excited states at CASPT2 level along the TD-DFT dynamic, highlighting the one with the highest overlap to the TD-DFT active state; (D) Oscillator strengths of the two lowest excited states at CASPT2 level over the TD-DFT dynamic, highlighting the one with the highest overlap to the TD-DFT active state. (E) Absolute value of the wavefunction overlap of the first two CASPT2 excited states with the TD-DFT active state. (F) Energy difference between active and ground state, computed at each level of theory. A fixed shift has been applied to account for the TDDFT overestimation of the $\pi\pi^*$ state energy. The line thickness in (C) and (D) is proportional to the projection of the TDDFT active state onto the CASPT2 manifold (E).

# Sample 7

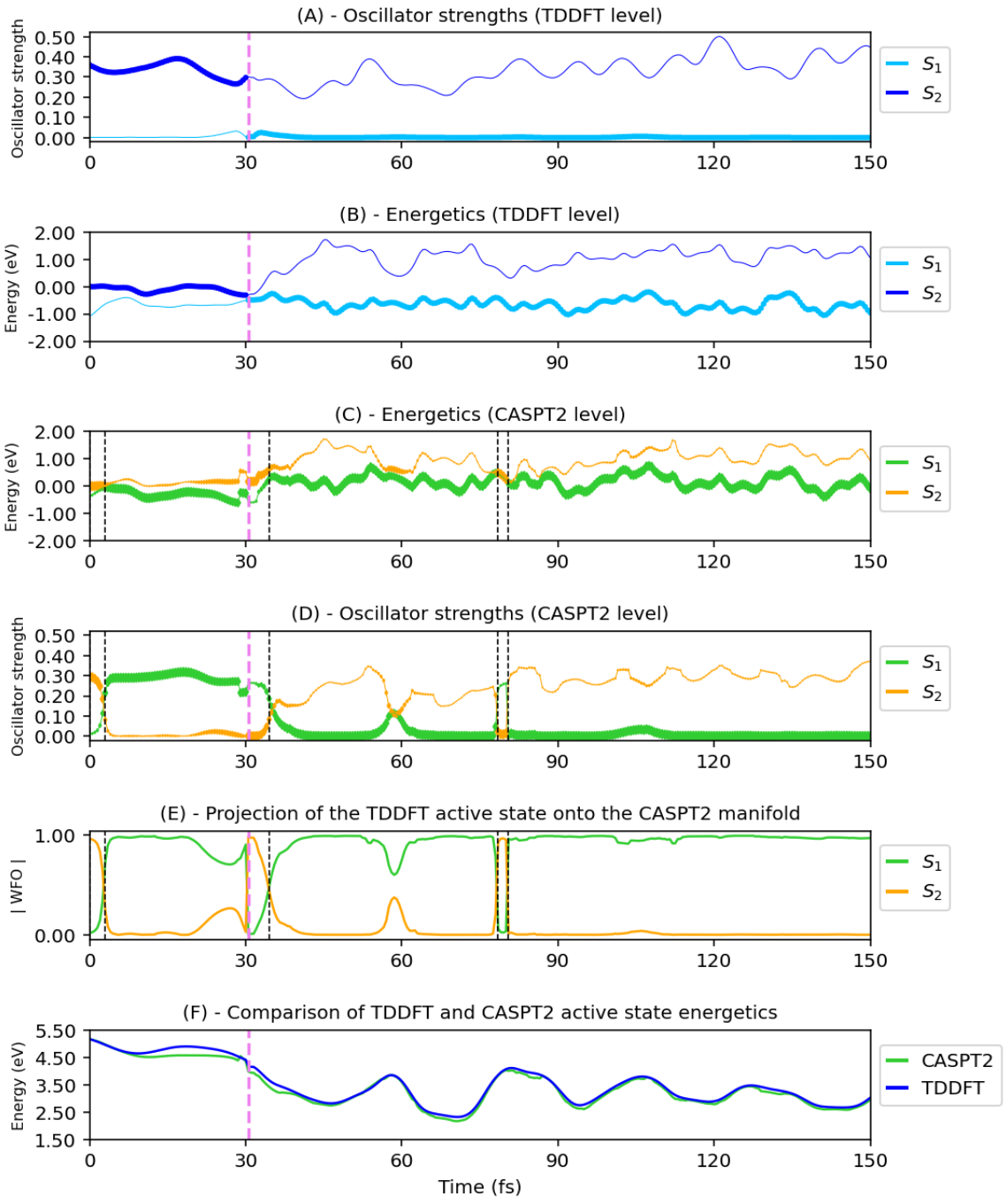


Supplementary Figure 7: Sample 7 - (A) Oscillator strengths of the two lowest excited states over the TD-DFT dynamic, highlighting the active one. (B) Energy of the three lowest excited states over the TD-DFT dynamic, highlighting the active one. (C) Energy of the two lowest excited states at CASPT2 level along the TD-DFT dynamic, highlighting the one with the highest overlap to the TD-DFT active state. (D) Oscillator strengths of the two lowest excited states at CASPT2 level over the TD-DFT dynamic, highlighting the one with the highest overlap to the TD-DFT active state; (E) Absolute value of the wavefunction overlap of the first two CASPT2 excited states with the TD-DFT active state. (F) Energy difference between active and ground state, computed at each level of theory. A fixed shift has been applied to account for the TDDFT overestimation of the $\pi\pi^*$ state energy. The line thickness in (C) and (D) is proportional to the projection of the TDDFT active state onto the CASPT2 manifold (E).

# Sample 8

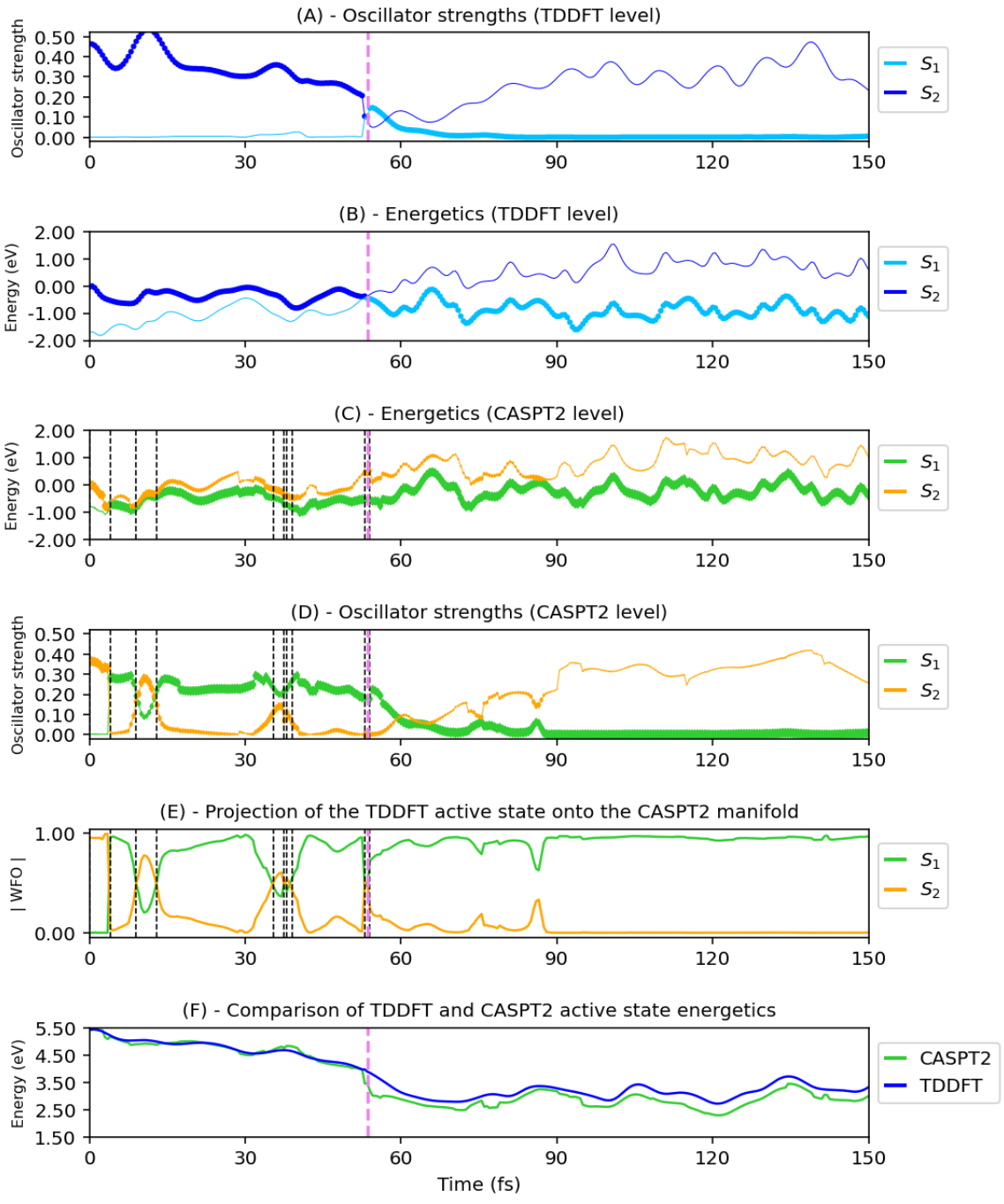


Supplementary Figure 8: Sample 8 - (A) Oscillator strengths of the two lowest excited states over the TD-DFT dynamic, highlighting the active one. (B) Energy of the three lowest excited states over the TD-DFT dynamic, highlighting the active one. (C) Energy of the two lowest excited states at CASPT2 level along the TD-DFT dynamic, highlighting the one with the highest overlap to the TD-DFT active state; (D) Oscillator strengths of the two lowest excited states at CASPT2 level over the TD-DFT dynamic, highlighting the one with the highest overlap to the TD-DFT active state. (E) Absolute value of the wavefunction overlap of the first two CASPT2 excited states with the TD-DFT active state. (F) Energy difference between active and ground state, computed at each level of theory. A fixed shift has been applied to account for the TDDFT overestimation of the $\pi\pi^*$ state energy. The line thickness in (C) and (D) is proportional to the projection of the TDDFT active state onto the CASPT2 manifold (E).

# Sample 9

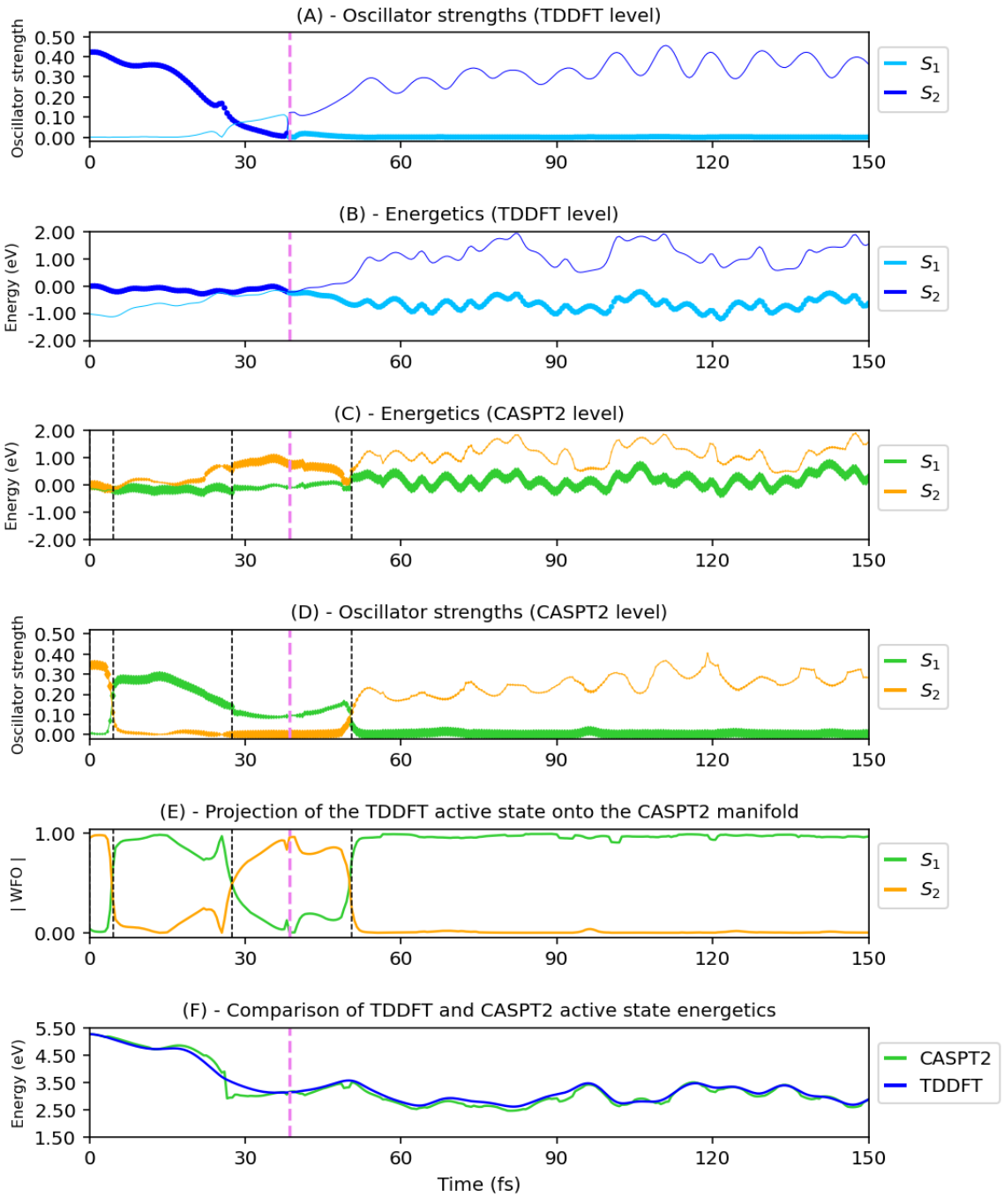


Supplementary Figure 9: Sample 9 - (A) Oscillator strengths of the two lowest excited states over the TD-DFT dynamic, highlighting the active one. (B) Energy of the three lowest excited states over the TD-DFT dynamic, highlighting the active one. (C) Energy of the two lowest excited states at CASPT2 level along the TD-DFT dynamic, highlighting the one with the highest overlap to the TD-DFT active state; (D) Oscillator strengths of the two lowest excited states at CASPT2 level over the TD-DFT dynamic, highlighting the one with the highest overlap to the TD-DFT active state. (E) Absolute value of the wavefunction overlap of the first two CASPT2 excited states with the TD-DFT active state. (F) Energy difference between active and ground state, computed at each level of theory. A fixed shift has been applied to account for the TDDFT overestimation of the $\pi\pi^*$ state energy. The line thickness in (C) and (D) is proportional to the projection of the TDDFT active state onto the CASPT2 manifold (E).

# Sample 10

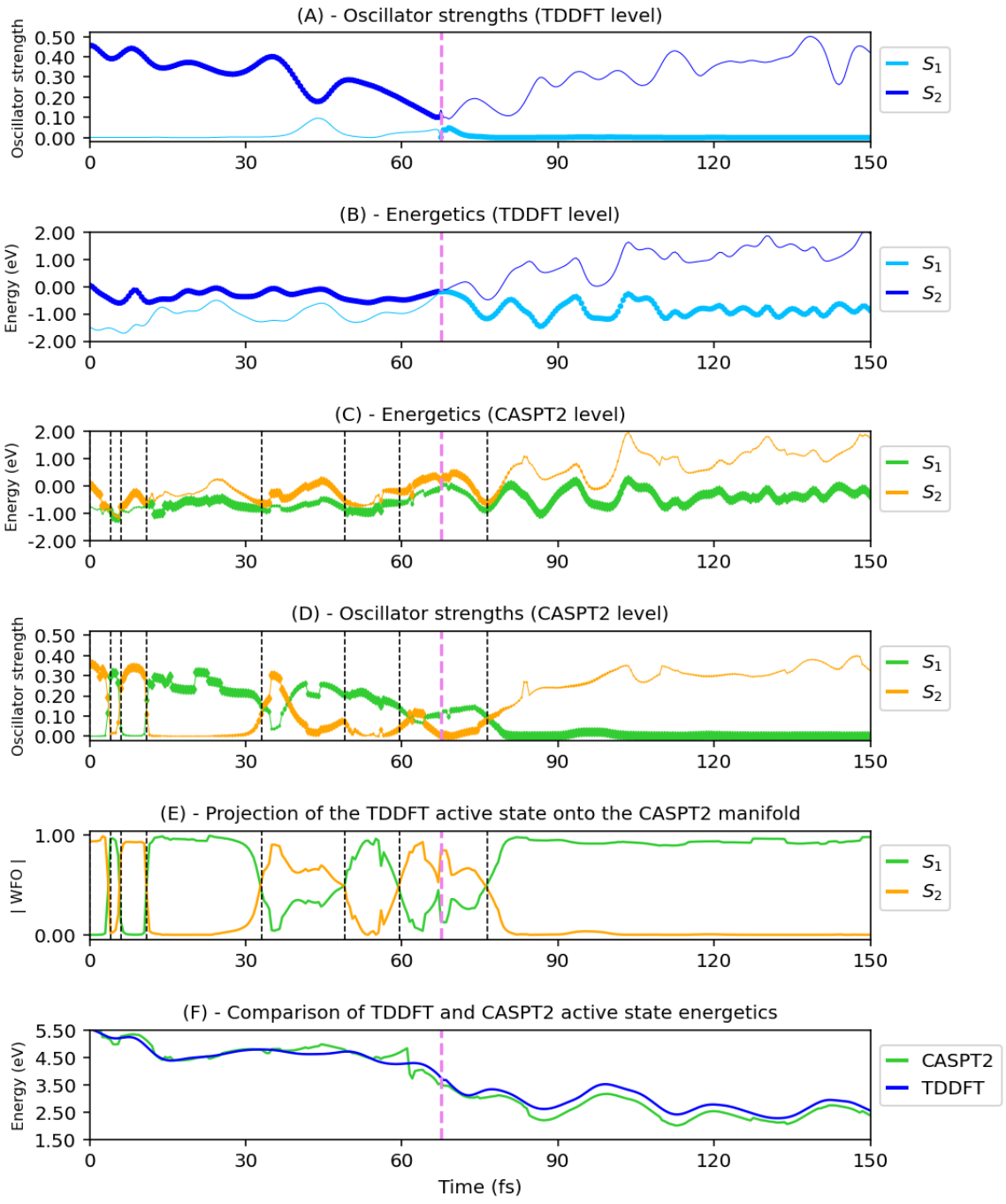


Supplementary Figure 10: Sample 10 - (A) Oscillator strengths of the two lowest excited states over the TD-DFT dynamic, highlighting the active one. (B) Energy of the three lowest excited states over the TD-DFT dynamic, highlighting the active one. (C) Energy of the two lowest excited states at CASPT2 level along the TD-DFT dynamic, highlighting the one with the highest overlap to the TD-DFT active state; (D) Oscillator strengths of the two lowest excited states at CASPT2 level over the TD-DFT dynamic, highlighting the one with the highest overlap to the TD-DFT active state. (E) Absolute value of the wavefunction overlap of the first two CASPT2 excited states with the TD-DFT active state. (F) Energy difference between active and ground state, computed at each level of theory. A fixed shift has been applied to account for the TDDFT overestimation of the $\pi\pi^*$ state energy. The line thickness in (C) and (D) is proportional to the projection of the TDDFT active state onto the CASPT2 manifold (E).

# Sample 11

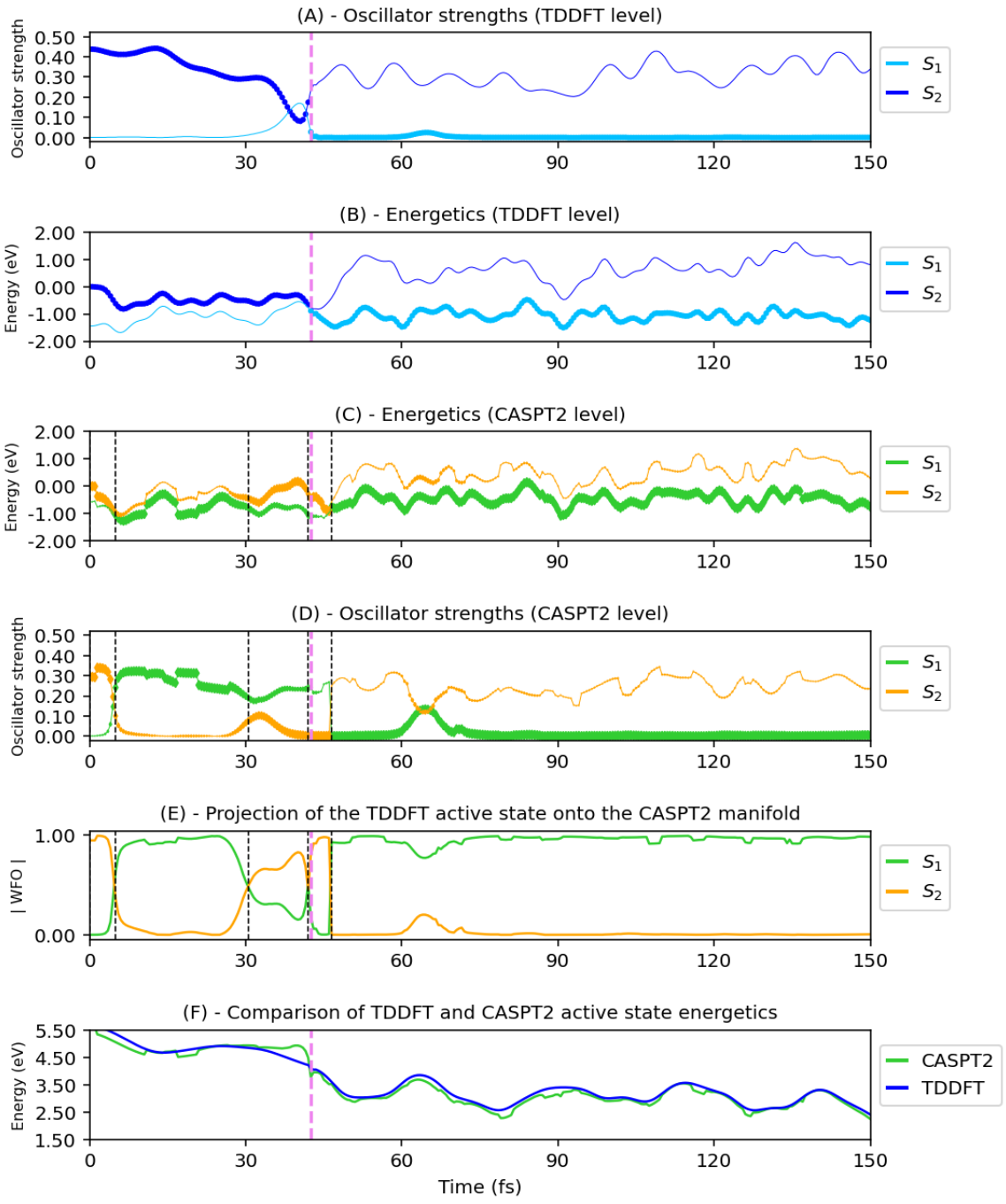


Supplementary Figure 11: Sample 11 - (A) Oscillator strengths of the two lowest excited states over the TD-DFT dynamic, highlighting the active one. (B) Energy of the three lowest excited states over the TD-DFT dynamic, highlighting the active one. (C) Energy of the two lowest excited states at CASPT2 level along the TD-DFT dynamic, highlighting the one with the highest overlap to the TD-DFT active state; (D) Oscillator strengths of the two lowest excited states at CASPT2 level over the TD-DFT dynamic, highlighting the one with the highest overlap to the TD-DFT active state. (E) Absolute value of the wavefunction overlap of the first two CASPT2 excited states with the TD-DFT active state. (F) Energy difference between active and ground state, computed at each level of theory. A fixed shift has been applied to account for the TDDFT overestimation of the $\pi\pi^*$ state energy. The line thickness in (C) and (D) is proportional to the projection of the TDDFT active state onto the CASPT2 manifold (E).

# Sample 12

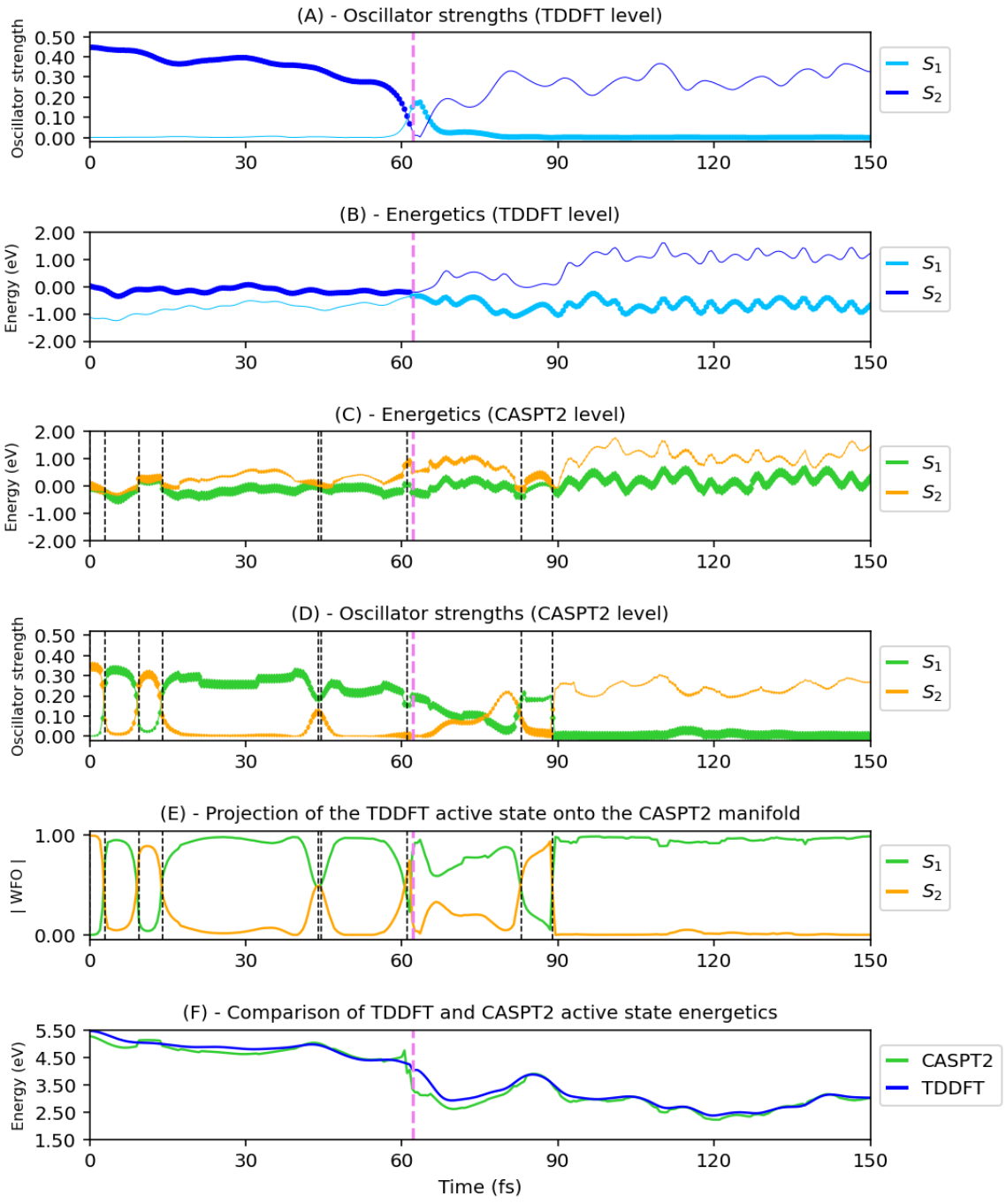


Supplementary Figure 12: Sample 12 - (A) Oscillator strengths of the two lowest excited states over the TD-DFT dynamic, highlighting the active one. (B) Energy of the three lowest excited states over the TD-DFT dynamic, highlighting the active one. (C) Energy of the two lowest excited states at CASPT2 level along the TD-DFT dynamic, highlighting the one with the highest overlap to the TD-DFT active state; (D) Oscillator strengths of the two lowest excited states at CASPT2 level over the TD-DFT dynamic, highlighting the one with the highest overlap to the TD-DFT active state. (E) Absolute value of the wavefunction overlap of the first two CASPT2 excited states with the TD-DFT active state. (F) Energy difference between active and ground state, computed at each level of theory. A fixed shift has been applied to account for the TDDFT overestimation of the $\pi\pi^*$ state energy. The line thickness in (C) and (D) is proportional to the projection of the TDDFT active state onto the CASPT2 manifold (E).

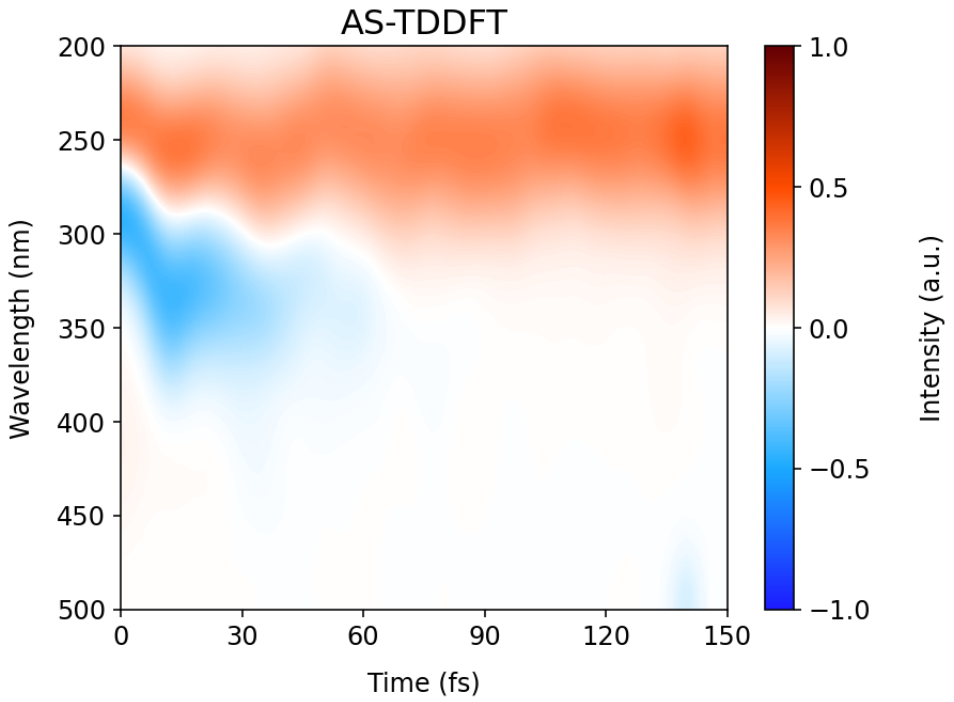


Supplementary Figure 13: Simulated transient absorption spectrum of AcAc obtained through averaging of 50 excited state trajectories. The signal at higher energy (dark-orange) is assigned to excited state absorption (ESA), while the one at lower energy (blue) is assigned to stimulated emission (SE) from the active state to the ground state. Ground state bleaching (GSB) is not included.

Supplementary Table 1: Energies of the first two excited states alongside their energy difference, computed at the Franck-Condon point for different TDDFT functionals and for CASPT2, where the latter is used as a reference for evaluating the functionals' correctness.

| Level of theory | $E(S_1)$ (eV) | $E(S_2)$ (eV) | $\Delta$E ($S_2$-$S_1$) (eV) |
|---|---|---|---|
| CAM-B3LYP | 4.515 | 5.597 | 1.082 |
| PBE0 | 4.385 | 5.563 | 1.178 |
| LC-wHPBE | 4.618 | 5.652 | 1.035 |
| M06 | 4.342 | 5.573 | 1.230 |
| XMS-24-CASPT2(10,8) | 4.223 | 4.517 | 0.294 |